SIMB Society for Industrial Microbiology and Biotechnology

Journal of Industrial Microbiology and Biotechnology, 2022, 49, kuac006

https://doi.org/10.1093/jimb/kuac006
Advance access publication date: 8 March 2022
Biocatalysis – Original Paper

Quantitative ^{1}H-NMR analysis reveals steric and electronic effects on the substrate specificity of benzoate dioxygenase in *Ralstonia eutropha* B9

James S. Bent, Zachary T. Clark, Jonathan A. Collins

Department of Chemistry, Whitman College, 345 Boyer Avenue, Walla Walla, WA 99362, USA
Correspondence should be addressed to: Jonathan A. Collins. Phone: +1-509-527-5181. E-mail: collinja@whitman.edu

Abstract: The *cis*-dihydroxylation of arenes by Rieske dearomatizing dioxygenases (RDDs) represents a powerful tool for the production of chiral precursors in organic synthesis. Here, the substrate specificity of the RDD benzoate dioxygenase (BZDO) in *Ralstonia eutropha* B9 whole cells was explored using quantitative ^{1}H nuclear magnetic resonance spectroscopy (q^{1}H-NMR). The specific activity, specific carbon uptake, and regioselectivity of the dihydroxylation reaction were evaluated in resting cell cultures for a panel of 17 monosubstituted benzoates. Two new substrates of this dioxygenase system were identified (2-methyl- and 3-methoxybenzoic acid) and the corresponding *cis*-diol metabolites were characterized. Higher activities were observed for benzoates with smaller substituents, predominantly at the 3-position. Elevated activities were also observed in substrates bearing greater partial charge at the C-2 position of the benzoate ring. The regioselectivity of the reaction was directly measured using q^{1}H-NMR and found to have positive correlation with increasing substituent size. These results widen the pool of *cis*-diol metabolites available for synthetic applications and offer a window into the substrate traits that govern specificity for BZDO.

Keywords: Reiske dearomatizing dioxygenase, Benzoate dioxygenase, *Ipso*,*ortho*-Dihydrodiols, *Ralstonia eutropha* B9, Substrate specificity

Introduction

The Rieske dearomatizing dioxygenases (RDDs) are a class of enzymes that have featured prominently at the interface between biocatalysis and synthetic organic chemistry (Barry & Challis, 2013). These dioxygenases are so named because they contain a Rieske [2Fe–2S] cluster and a nonheme mononuclear Fe catalytic center (Ferraro et al., 2005). Since their initial discovery as components in benzene metabolism by *Pseudomonas putida* (Gibson et al., 1968), RDD enzymes have been found within hydrocarbon-degrading pathways for a number of soil bacteria (Ferraro et al., 2005). They share the common trait of achieving dearomatization through a *cis*-dihydroxylation of the aromatic ring using an equivalent of molecular oxygen (Fig. 1). This activates the ring for further degradation, making these dioxygenases potentially useful as bioremediation agents (Tan & Parales, 2016).

The dihydroxylation reaction is often regio- and stereoselective, leading to the formation of chiral dihydrodiols. This has given rise to sustained interest in these metabolites as building blocks in the synthesis of important small molecules (Hudlicky, 2018; Lewis, 2015). The *ortho*,*meta* *cis*-dihydrodiols (**2**) are typically derived from toluene (TDO), naphthalene (NDO), and biphenyl dioxygenases (BPDOs) expressed in whole cells (Wackett, 2002). These RDDs generally have broad substrate scopes. Over 420 distinct substrates have been identified for these systems to date (Hudlicky, 2018). In addition to diol formation, these enzymes have also demonstrated the ability to catalyze reactions such as benzylic oxidation, *N*-/*O*-dealkylation, and formation of chiral sulfoxides from sulfides (Johnson, 2004). These non-native activities further broaden their potential in synesthetic and bioremediation applications.

By comparison, the *ipso*,*ortho* *cis*-dihydrodiols (**3**) have been applied far less frequently (Hudlicky, 2018; Lewis, 2014). These metabolites can be accessed through the 1,2-dihydroxylation of benzoic acids using toluate (TADO) and benzoate dioxygenases (BZDOs) (Lewis, 2015; Whited et al., 1986). The most widely applied system for production of *ipso*,*ortho* *cis*-dihydrodiols is *Ralstonia eutropha* B9 (formerly *Alcaligenes eutrophus*, now *Cupriavidus necator*) whole cells expressing BZDO (Reiner & Hegeman, 1971). This mutant strain produces an inactive form of dihydrodihydroxybenzoic acid (DHB) dehydrogenase (conversion of **3** to **5**), which allows for accumulation of the benzoate diol (**3**) (Johnson & Stanier, 1971). The Myers group was one of the first to apply the whole-cell system to production of **3** on a preparative scale (270 g), using it to synthesize a number of highly functionalized derivatives (Myers et al., 2001). Since then, *R. eutropha* B9 has been employed in several notable synthetic applications. Some examples include preparation of tetracycline antibiotics (Charest et al., 2005), novel heterocyclic scaffolds using cycloadditions (Adams et al., 2014; Fischer et al., 2010; Jenkins et al., 1995; Pazos et al., 2015), epoxiquinol natural products (Collins et al., 2019), pleiogenone A (Froese et al., 2016), and grandifloracin derivatives (Alexander et al., 2020). Despite the recent surge in interest in these *ipso*,*ortho* *cis*-dihydrodiols, applications of non-native substrates of BZDO are still rare (Nash et al., 2017). This is perhaps unsurprising given the scarcity of information about the substrate scope of BZDO.

This dearth of information on BZDO substrate specificity is in part due to the difficulty of isolating and characterizing metabolites on small scale. Diols of both types (**2** and **3**) tend to rearomatize to the corresponding phenol through a dehydration

Received: October 5, 2021. **Accepted:** February 20, 2022.

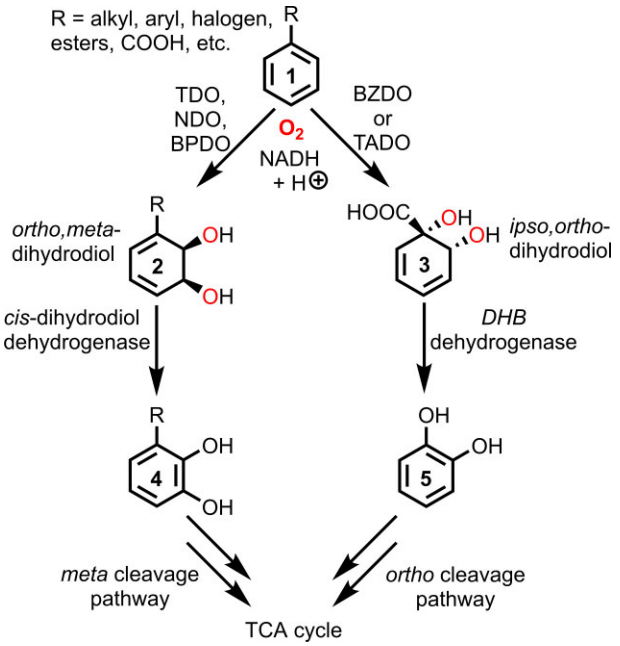

Fig. 1 Formation of *ortho*,*meta*- and *ipso*,*ortho*-dihydrodiols by Rieske dearomatizing dioxygenases and their role in arene metabolism in bacteria.

reaction when exposed to elevated temperature and acidic pH. This is especially true for the *ipso*,*ortho cis*-dihydrodiols (**3**) derived from benzoic acids, which require that the pH be adjusted to 3–4 before efficient extraction during downstream processing. In cases where multiple metabolites are possible (2- or 3-substituted benzoates), isolation can degrade minor and/or less stable products, leading to the reporting of skewed isomeric ratios (Reineke et al., 1978). Less invasive methods such as high-performance liquid chromatography (HPLC), UV/vis, and stopped-flow single-turnover kinetics of isolated enzymes can measure biotransformation activity but fail to provide sufficient characterization of metabolites (chemo- and regioselectivity). This lack of clarity can make it difficult to extract important mechanistic information and can hamper application of metabolites derived from non-native substrates. We have sought to overcome these limitations by employing quantitative ^{1}H nuclear magnetic resonance spectroscopy (q^{1}H-NMR) to measure the biocatalytic activity of *R. eutropha* B9 whole cells expressing BZDO. While the application of q^{1}H-NMR as a method for the study of enzyme-catalyzed reactions (Brecker & Ribbons, 2000) and biochemical pathways (Barding et al., 2012; Simmler et al., 2014) is known, its use to directly explore the substrate scope of RDDs is not. Here, it has allowed determination of the specific activity, carbon uptake, and the regioselectivity of the dioxygenase reaction for a variety of monosubstituted benzoates, thereby providing new insight into the factors governing the substrate specificity of this biotransformation and elucidating new diol frameworks for potential application in synthesis.

Materials and Methods

Bacterial Strains and General Cultivation

The *R. eutropha* B9 mutant was derived from *R. eutropha* 335 (ATCC 17697) (Johnson & Stanier, 1971) and kindly provided by Marko Mihovilovic, Vienna University of Technology. LB (Miller) (Sambrook & Russell, 2001) agar plates were streaked with glycerol freezer stocks of *R. eutropha* B9 and grown for 2 days at 30°C. A preculture consisting of LB medium (5 ml) was inoculated with a single colony and cultivated overnight (~12 hr) at 30°C and 200 rpm. A portion of this small culture (1.2 ml) was then added to a 500 ml flask containing 100 ml Hutner's mineral base (HMB) medium (Fischer et al., 2010; Myers et al., 2001) that had been complemented with 40 mM sodium succinate (final OD_{600} = 0.019). The culture was grown for 12 hr at 30°C and 200 rpm before an aliquot (13.5 ml) was taken and used to inoculate a 5 l RALF bioreactor (Bioengineering) containing 3 l HMB and 40 mM sodium succinate (final OD_{600} = 0.024). The batch was cultivated at 30°C, pH 7.4, 300 rpm agitation, and 1.0 l/min aeration. The pH was maintained at 7.4 by addition of concentrated ammonium hydroxide and 30% (vol/vol) phosphoric acid. When the cells had reached an OD_{600} = 2.25 (10 hr), sodium succinate (50 ml, 1.25 M) was added and the culture was induced with sodium benzoate (15 ml, 2.0 M, 10 mM final concentration). After complete consumption of the benzoate, as indicated by a rapid spike in pO_2 after 2.5 hr, an additional portion (7.5 ml, 2 M) was added, along with sodium succinate (30 ml, 1.25 M). Stirring was increased to 500 rpm and aeration to 2.0 l/min. After an additional 2 hr of cultivation, the OD_{600} had reached ~5, at which point the cells were harvested by centrifugation (Allegra™ 25R centrifuge, 8618 × *g*, 15 min) and washed twice with sodium phosphate buffer (50 mM, pH 6.8). The cell pellets were combined and resuspended a final time in phosphate buffer to an OD_{600} = 15.

Substrate Screening Experiments Using Resting Cells

Suspensions of resting cells (OD_{600} = 15 in phosphate buffer) were divided into 100 ml portions in 500 ml baffled shaking flasks and complemented with sodium succinate (1.6 ml, 1.25 M). The resting cultures were placed in an orbital shaker and allowed to recover for 20 min. at 30°C and 200 rpm. Substituted benzoate substrates were added to each shaking flask to reach a final concentration of 10 mM. In cases where the substrates displayed reduced solubility in the phosphate buffer, they were first dissolved in a minimal amount of 6 M potassium hydroxide prior to introduction into the shaking flask. Ultrasonication was used to assist in dissolving the substrates as needed. A sample was taken directly after substrate addition and at 18 hr. The cells were removed via centrifugation (Eppendorf centrifuge 5415D, 9300 × *g*, 1 min) and the supernatant immediately frozen and stored at −20°C until analysis. Identified substrates were assayed a second time and in duplicate using the above procedure but with sampling at additional time points (0, 1, 2, 3, 6, and 18 hr).

Downstream Processing and q^{1}H-NMR Analysis of Resting Cell Cultures

Aqueous broth samples were thawed and allowed to come to room temperature. A 1000 μl aliquot of each sample was transferred to a fresh 1.5 ml microcentrifuge tube. To this aliquot was added 100 μl of a 100 mM benzene-1,3,5-tricarboxylic acid solution. The tubes were placed in a centrifugal vacuum concentrator (Thermo Scientific, Savant ISS110) and concentrated to dryness at 43°C (~5 hr). The salts were then dried over P_2O_5 under high vacuum overnight to remove residual water. Samples were then redissolved in 700 μl D_2O and transferred to NMR tubes (Wildman, Economy). Proton NMR spectra were acquired using a Bruker Ultrashield Plus 400 MHz instrument fitted with a 60-sample autochanger. The ^{1}H-NMR spectra were acquired using the following parameters: acquisition time of 4.89 s, relaxation delay of 1.00 s, 90° pulse width of 15.00 μs, 30° tip angle, 65k data points, and 128 scans at 298 K. Concentrations of substrates,

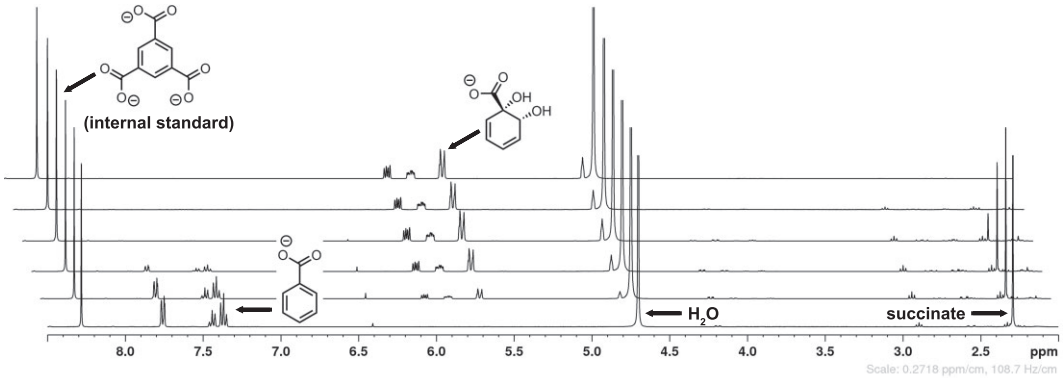

Fig. 2 Quantitative nuclear magnetic resonance spectroscopy (q^1H-NMR) spectra of the transformation of sodium benzoate over time with benzene-1,3,5-ticarboxylic acid as internal standard (10 mM). All spectra were acquired at 400 MHz in D_2O.

metabolites, and succinate were determined by comparison of their integrations with that of benzene-1,3,5-tricarboxylic acid (internal standard, 10 mM, 3H). Specific activity and carbon uptake values were calculated using g_{CDW}/l, which was determined by standard curve correlation to OD_{600} ($0.4065 \times OD_{600} = g_{CDW}/l$). All values were recorded in duplicate and reported as an average.

Identification of Metabolites

The ^{1}H-NMR spectra (described above) from the final time points (18 hr) were used for structural elucidation of the obtained metabolites. Where applicable, ^{19}F-NMR (376 MHz) was used for further characterization. The products were also confirmed by HPLC–mass spectrometry (MS). Aqueous broth samples were thawed, centrifuged (Eppendorf centrifuge 5415D, 13,400 × *g*, 10 min), and diluted 10:1 with water. HPLC (Agilent, USA), equipped with a C18 column (Supelco, 10 cm by 4.6 mm, 5 μm) was run at 0.8 ml/min flow rate using water–acetonitrile (7:3) containing 1.0% acetic acid (volume). The substrates and metabolites were detected by UV absorbance at 254 nm and MS (API-ES, negative polarity, Agilent, USA). Retention times of substrates were matched to those of authentic standards.

Computational Methods

Geometries for the 3-substituted benzoates were optimized using the ORCA 4.2.0 quantum chemistry program (Neese 2011, 2017). The M06-2X level of density functional theory (Zhao & Truhlar, 2008) and the def2-tzvp basis set were used for all calculations (Weigend & Ahlrichs, 2005). The conjugate base forms of the acids were used in the optimizations with the SMD quantum aqueous solvation model (Marenich et al., 2009). Hirshfeld partial charges were calculated at the same level of theory (Hirshfeld, 1977). Charges are reported as the net charge for the C(2)–H group. In cases where different C-2 positions existed (3-substituted benzoates), the value represents the average of the two C(2)–H groups. Van der Waal's volumes were calculated using MarvinSketch (version 21.4.0, ChemAxon)

Results

Evaluation of Native and Non-Native Substrates Using q^1H-NMR

The suitability of q^1H-NMR for the determination of BZDO activity in *R. eutropha* B9 was first examined using the native transformation. Resting cultures of *R. eutropha* B9 were treated with sodium benzoate at a 10 mM concentration. At various time points, aliquots of the culture were taken and used to prepare samples for ^{1}H-NMR analysis. The initial experiment relied on direct dilution of these aqueous samples with D_2O and dimethyl sulfoxide as an internal standard, but this resulted in spectra that were dominated by a large residual water peak. Solvent suppression routines were successful in reducing this peak, but they significantly increased the time needed to set up and process each experiment. Concentration of the aqueous biotransformation samples to their dried salts and direct analysis in D_2O greatly simplified the workflow and improved the overall throughput. Acquisition of ^{1}H-NMR spectra for each time point allowed monitoring of the biotransformation (Fig. 2).

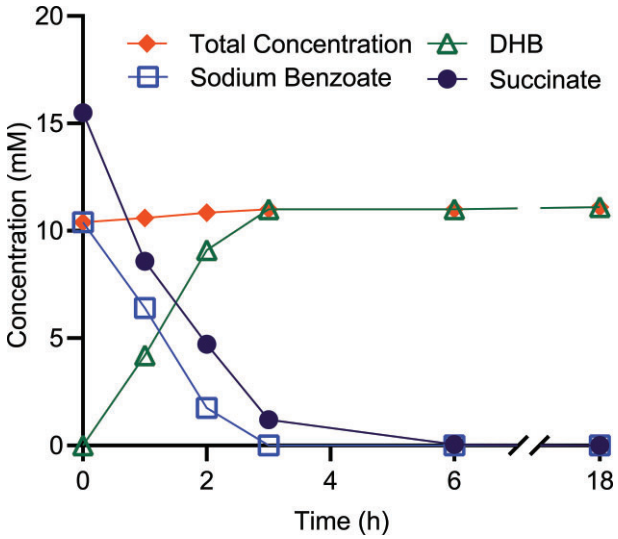

Fig. 3 Transformation of sodium benzoate, consumption of succinate, and production of dihydrodihydroxybenzoic acid (DHB) over time by *Ralstonia eutropha* B9 resting cells in 100 ml shaking flask cultures.

The native substrate (sodium benzoate) was rapidly transformed over the first three hours to give *ipso*,*ortho cis*-dihydrodiol **3**. Integration of a chemical shift corresponding to benzoic acid (7.79–7.34 ppm, 5H) relative to the internal standard (8.28 ppm, 3H, 10 mM) allowed a straightforward calculation of the benzoate concentration. The concentrations of diol metabolite **3** and succinate (carbon source) were likewise determined. The concentrations over time of biotransformation components are shown in Fig. 3.

Benzoate was rapidly transformed, falling from an initial concentration of 10.4 mM to full consumption by $t = 3$ hr. This corresponded to an increase in the formation of *cis*-dihydrodiol **3**.

Table 1. Specific Activity and Succinate Uptake by Resting Cultures of *Ralstonia eutropha* B9

Substrate	Specific activity[a] (μmol/min/g_{CDW})	Relative activity[b] (%)	Specific C uptake (succinate)[c] (μmol/min/g_{CDW})	Relative C uptake[d] (%)
Benzoate	12[e]	100	15[e]	100
2-Fluoro-	1.6	13	17	130
2-Chloro-	0[f]	0[f] (0[g])	–	–
2-Bromo-	0[f]	0[f] (0[h])	–	–
2-Iodo-	0[f]	0[f]	–	–
2-Methyl-	0.75	4.9 (0[g])	26	120
2-Methoxy-	0[f]	0[f]	–	–
3-Fluoro-	12	101 (40[i])	13	94
3-Chloro-	4.9	45 (15[g])	8.7	57
3-Bromo-	1.1	9.1 (8[j])	8.0	46
3-Iodo-	0[f]	0[f]	–	–
3-Methyl-	9.1	60.0 (24.6[g])	15	71
3-Methoxy-	0.7	5.54	16	94
4-Fluoro-	4.8	40.0 (40[i])	14	110
4-Chloro-	0[f]	0[f] (0.0775[g])	–	–
4-Bromo-	0[f]	0[f] (0[h])	–	–
4-Iodo-	0[f]	0[f]	–	–
4-Methyl-	0.51	3.3 (0.4[g])	7.2	34
4-Methoxy-	0[f]	0[f]	–	–

[a]Specific activity is defined as the quantity of benzoate transformed by 1 g cell dry weight (CDW) in 1 min.
[b]Activity is reported as percentage relative to the specific activity of the native substrate (benzoate) using the same batch of resting cells. Where available, literature values are reported in parentheses.
[c]Specific carbon uptake is defined as the quantity of succinate consumed by 1 g cell CDW in 1 min.
[d]Carbon uptake (succinate) is reported as percentage relative to the specific carbon uptake of resting cells during the transformation of the native substrate (benzoate).
[e]Indicates an average of benzoate standards from four different pools of resting cells.
[f]Indicates no conversion of substrate during initial screening.
[g](Knackmuss & Reineke, 1973).
[h](Reineke et al., 1978).
[i](Reiner & Hegeman, 1971).
[j](Reineke & Knackmuss, 1978).

Mass balance was well maintained throughout the transformation as evidenced by a steady total concentration (substrate + metabolite). This indicated that neither the substrate nor the metabolite was being appreciably retained by the cells. The uptake of succinate was also tracked from an initial concentration of 15.5 mM to 1.2 mM at t = 3 hr. From these data, the initial specific activity and carbon uptake rates were calculated (Table 1). Identical benzoate transformations were performed with each set of non-native substrate screens in order to establish benchmarks for BZDO activity and carbon uptake.

A panel of monosubstituted benzoic acids was screened for activity against BZDO in *R. eutropha* B9 resting cells. As with the native benzoate transformation, initial activity and carbon uptake were calculated from the linear portion of the plot (0–2 hr). At this point, substrate concentrations were high (~10 mM) and rates were assumed to be at or near maximum. For the purposes of comparison, the relative activity and carbon uptake of identified substrates were calculated based on the standard benzoate transformation (Table 1).

In general, the highest activities were observed for 3-substituted benzoates. The 3-fluorobenzoic acid displayed a rate of reaction comparable with that of the native substrate. Within the remaining 3-halogenated benzoates, the activity decreased down the group to iodine, where no activity was observed. The 3-methylbenzoic acid substrate also displayed a relatively high activity (~60% of native benzoate). The 3-methoxybezoic acid transformed, albeit at a significantly reduced rate. Relative carbon uptake was proportional to relative activity in the 3-substituted series, except in the case of 3-methoxybenzoic acid. Here the relative carbon uptake was similar to the native substrate while maintaining a fraction of the activity. By comparison, the 2- and 4-substituted benzoates were tolerated far less by the BZDO system. In both cases, the only substrates with measured activity were the fluoro- and methylbenzoic acids. The lower activity of these substrates provided a good opportunity to test the limits of the sensitivity of this q^{1}H-NMR method. Changes in substrate/metabolite concentration of ≥0.1 mM (1% change) were routinely recorded. Concentrations as small as 0.05 mM were observed, but they were not uniformly reproducible across the substrate panel. In the 4-substituted series, the carbon uptake again tracked with activity in the whole-cells. This contrasts with the large carbon uptake (relative to activity) in the 2-substituted series.

Determination of Regioselectivity and Off-Target Transformations Using q ^{1}H-NMR

The reported activities were based on consumption of the substrate in the resting cell cultures. One of our motivations for applying q^{1}H-NMR analysis to this system was its ability to simultaneously provide structural information on the obtained metabolites. This is especially critical in cases where it is possible to form regioisomeric mixtures of products. Analysis of ^{1}H-NMR spectra of 3-substituted benzoates indicated that the metabolites were obtained as mixtures of 3- and 5-substituted *ipso,ortho cis*-dihydrodiols (Fig. 4). The exception was 3-methoxybenzoic acid, which yielded only the 3-substituted diol.

In all instances, the 3-substituted *ipso,ortho cis*-dihydrodiols were favored over the 5-substituted metabolites. The ratios were assigned by examining coupling patterns of the alkene protons in the ^{1}H-NMR (Figs S6–S15). The least selective substrate was

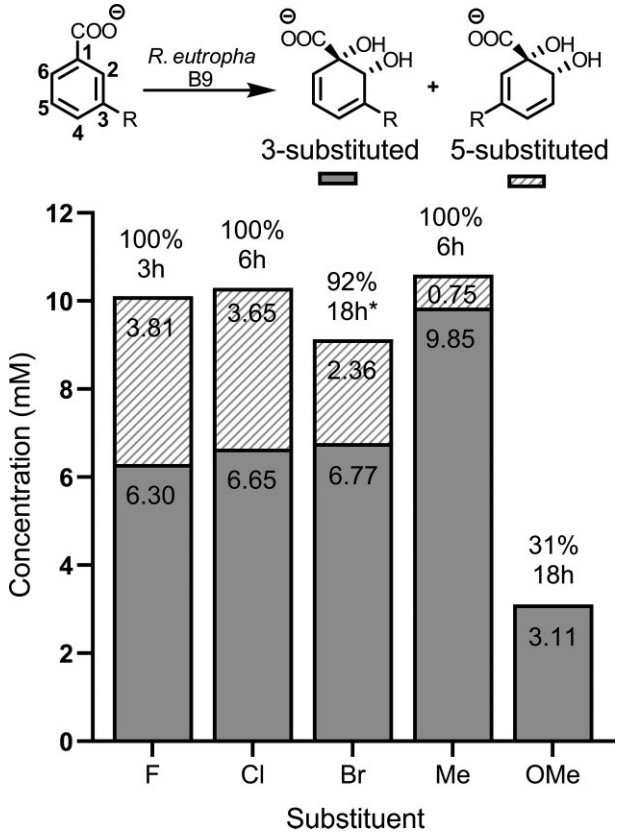

Fig. 4 Final concentrations of 3/5-substituted metabolites from transformation of 3-substituted benzoates using *Ralstonia eutropha* B9 resting cells. Final percentage conversion and time required are listed above each column. Cases marked with an (*) indicating that the reaction was stopped after 18 hr.

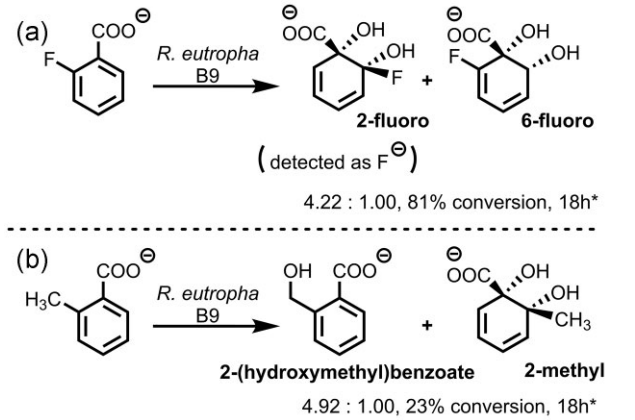

Fig. 5 Regioselectivity and metabolites from oxidation of 2-substituted benzoates by *Ralstonia eutropha* B9 resting cells (benzoate dioxygenase, BZDO). (a) 2-Fluorobenzoic acid: the 2-fluoro metabolite was detected as fluoride in solution (^{19}F-NMR) following elimination and catabolism of the resulting catechol (Figure S2). (b) 2-Methylbenzoic acid. (*) indicates that the reaction was stopped after 18 hr.

3-fluorobenzoic acid, yielding a 1.65:1.00 ratio of 3/5-substituted diols. Assignment of the isomeric ratio of the 3/5-fluoro benzoate metabolites was complicated by the added proton–fluorine coupling. Heteronuclear decoupling of the fluorine allowed for unambiguous assignment of two isomers (Fig. S6). The presence of the fluorine atom also allowed for characterization of the metabolites using ^{19}F-NMR (Fig. S7). This provided a complementary method for determining the regioselectivity of fluorinated metabolites. The transformation became more selective as substitution moved down the halogen group. This was associated with a decrease in overall rate of the reaction (Table 1 and Fig. 4). The 3-methylbenzoic acid was the second most selective substrate, providing a >13:1 ratio of 3/5-substituted products.

The 2-substituted benzoate substrates also allow for formation of two different isomers (Fig. 5). Examination of the ^{1}H and ^{19}F-NMR spectra of the 2-fluorobenzoic acid transformation initially revealed only the 6-fluoro metabolite. This was accompanied by a significant loss of mass balance for the reaction (Fig. S3). Over the course of the transformation, the concentration of substrate decreased by 8.10 mM, while the 6-fluoro metabolite reached only a 1.55 mM concentration. The ^{19}F-NMR contained a singlet at −122 ppm, which corresponded to free fluoride in solution. Integration of this peak accounted for the missing mass. This was in good accordance with Reineke, who had previously reported the spontaneous decarboxylative defluorination of the 2-fluoro metabolite to catechol, followed by complete catabolism by the whole cells via the 3-oxoadipate pathway (Reineke & Knackmuss, 1988). The enzymatic oxidation of 2-methylbenzoic acid yielded a mixture of 2-methyl diol and the benzylic oxidation products. The latter was readily identified by the appearance of a 2H singlet at 4.64 ppm, which corresponded to the benzylic methylene. This was later matched to authentic 2-(hydroxymethyl)benzoate (NMR, LCMS).

Discussion

Investigation of BZDO activity on non-native substrates is a powerful tool for probing the mechanistic details of this RDD. This is especially true in this case, where a lack of crystallographic information about the enzyme prevents detailed theoretical investigations. Early studies of the substrate scope of *R. eutropha* B9 served to establish some general trends for the RDD system: (1) *meta*-substituted benzoates are favored over *ortho*/*para* and (2) larger substituents correlate with lower activities (see Table 1 and reference therein). Our results are in general agreement with these previously identified trends but the choice of q^{1}H-NMR as a primary method of analysis has afforded several advantages. The strength of NMR as a tool for qualitative structural determination facilitated both the identification of two new substrates (2-Me and 3-OMe) and the characterization of the corresponding metabolites. The ability to quantitatively assess the transformation using the same measurement provided a convenient method for determining the activity and regioselectivity of the biotransformation. This led to the identification of sterics as a primary factor governing substrate specificity and the correlation of electron-donating substituents with greater activity of the resting whole cells. The various aspects of the processing of monosubstituted benzoates by BZDO *R. eutropha* B9 are discussed here.

The use of q^{1}H-NMR allowed for the establishment of 2-methylbenzoate as a substrate. Previously, it had been evaluated but was reported as having no activity (Knackmuss & Reineke, 1973). This is perhaps unsurprising given its low activity and the limitations of the analytical method employed at the time (UV/vis absorption, etc.). The structural information provided by NMR also allowed for identification of 2-(hydroxymethyl)benzoate as the primary metabolite. Benzylic oxidation is known for some RDDs (Johnson, 2004), but to our knowledge this is the first report of this activity in *R. eutropha* B9. Benzylic oxidation was not observed for any other methyl-substituted substrates, so it is likely that this

off-target activity is facilitated by the proximity of the 2-methyl group to the catalytic mononuclear iron center of BZDO.

With the 3-substituted benzoates, quantitative ^{1}H-NMR analysis was also able to identify significant differences between previously reported activities and those presented here. In almost every case, we report higher maximum relative rates. This discrepancy could be due to several factors. First, our relative rates are derived from specific activities based on grams cell dry weight (gCDW) as a measure of biomass. Previous values were based on estimations of aqueous protein content (Reineke & Knackmuss, 1978). Specific activity has been reported for a BZDO expressed in growing *P. putida* KTSY01 whole cells (Sun et al., 2008). There, Chen reported a specific activity (formation of **3**) of 0.09 mmol/gCDW/L/h. A comparison to our obtained value of 0.72 mmol/gCDW/L/h indicates that *R. eutropha* B9 resting cells are a highly active platform for this transformation, though this is significantly below the 1.2 mmol/gCDW/L/h reported for their recombinant *P. putida* KT2442 (pSYM01). Second, the previous activity assays with *R. eutropha* B9 whole cells were conducted using relatively dilute substrate concentrations (i.e. ≤2 mM). This could lead to a failure to achieve V_{max} with respect to the non-native substrates. It is also possible that mass transfer into (and out of) the whole-cell system is a limiting factor at these lower concentrations. Substrate concentrations of 10 mM were selected here because it was the maximum allowed by the whole-cell system. Substrate concentrations approaching 15 mM were generally accompanied by signs of cell toxification (e.g. reduced optical density and activity). At 10 mM substrate, we observed relative rates for 3-substituted benzoates (e.g. F, Me, and Cl) that were remarkably close to the relative turnover numbers for isolated BZDO (Wolfe et al., 2002). This confirmed that observed rates were indeed maximums and that system was not mass transfer limited on substrate.

Quantitative ^{1}H-NMR also provided rapid analysis of regioisomeric mixtures formed in transformations of 3-substituted benzoates. Early investigations of these substrates identified the presence of the 3/5-regioisomeric mixtures but either failed to quantify them (Reiner & Hegeman, 1971) or misassigned the 5-substituted isomer as the major component (Knackmuss & Reineke, 1973). The use of q^{1}H-NMR allowed both the identification and quantification of the regioisomers using straightforward analysis of scalar coupling and integration of the chemical shifts. After compensating for previous misassignments, our determined ratio for the 3/5-Cl metabolites compares closely with that of Knackmuss and Reineke (1.82:1.00 vs. 2:1). The same does not hold true for the 3/5-Me ratio, which they report as 7:1 (compared with our 13:1 ratio). Isolation and derivatization of the metabolites allowed characterization of the 3/5-Cl, Br, Me, and F regioisomers, but failed to provide ratios (Reineke et al., 1978). Even if ratios had been reported, the number of synthetic manipulations would have almost certainly skewed them toward enrichment of the major isomer (Hudlicky, 1996). This is especially true given the tendency for arene *ipso*,*ortho* diols to undergo dehydrative rearomatization, either as a deliberate derivatization during characterization or inadvertently during isolation under acidic conditions (Lewis, 2014). Here again, the presented q^{1}H-NMR method circumvents these obstacles by allowing direct analysis of the metabolites without isolation or derivatization. The transformation of 3-bromobenzoic acid by *R. eutropha* B9 to the 3/5-Br *ipso*,*ortho*-diol metabolites has been investigated in detail (Griffen et al., 2011). This study is notable for its robust characterization of the 3/5-Br metabolites (including determination of absolute stereochemical configuration) and for being the first true synthetic application of non-native arene diols from *R. eutropha* B9. The ratio of the crude 3/5-Br isomers is reported as >10:1 following acidic extraction. This contrasts with our ratio of 2.87:1.00, obtained from direct analysis using q^{1}H-NMR. While important for synthetic investigations, this serves to highlight the unreliability of using ratios measured from isolated *ipso*,*ortho* diols for making specific inferences about the regioselectivity of the BZDO system.

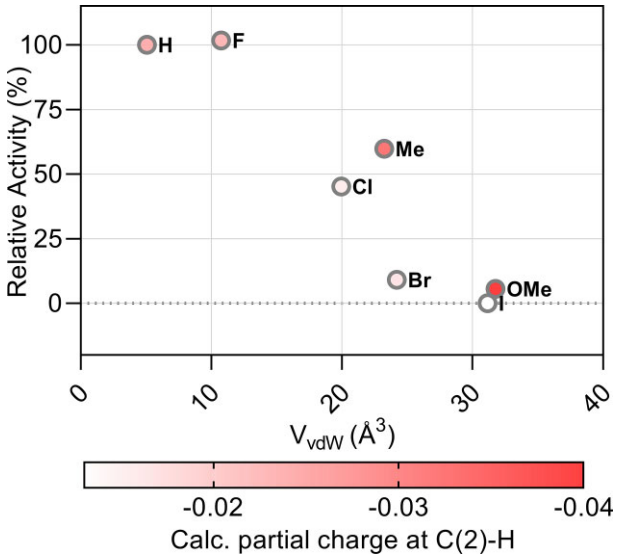

Fig. 6 Correlation between relative activity of 3-substituted benzoates and size. Activity is reported as percentage relative to that of native substrate (sodium benzoate). Size is reported as van der Waals volume (V_{vdW}) in units of cubic angstrom. Electronic contribution of each substrate is reported as the average Hirshfeld partial group charge at C(2)–H.

Early on, attempts were made by Knackmuss to correlate RDD activity on 3-substituted benzoates to substituent effects (Reineke & Knackmuss, 1978). Based on a proposed mechanism of electrophilic substitution of the ring, Hammett σ values were selected to represent substituent electronic effects for RDD activity involving *P. putida* mt-2 and *Pseudomonas* sp. B13. Electron-withdrawing groups were generally correlated to lower relative activities for *P. putida* mt-2, while no correlation was found for *Pseudomonas* sp. B13. Extraction of more specific relationships from these data is made somewhat challenging by the inclusion of the relative rates from all reported 2-, 3-, 4-, and di-substituted substrates. The RDDs expressed in these two organisms also have dramatically different substrate specificities from BZDO in *R. eutropha* B9, making direct comparison difficult. Additionally, the results from *P. putida* mt-2 appear to be derived from a mixture of RDDs: a genomically encoded BZDO (Wolfe et al., 2002), and a TOL plasmid-based toluate dioxygenase (TADO) (Ge et al., 2002). More recent mechanistic investigations of the substrate specificity of BZDO from *P. putida* mt-2 have suggested a positive correlation between activity and increased electron density at the C(2)–H group of sterically unhindered substrates (Rivard et al., 2015). This further supports a connection between substituent-based electronic effects and activity in these RDDs.

A plot of relative activity versus substituent size (van der Waal's volume, V_{vdW}) for the 3-substituted benzoates gave a negative trend (Fig. 6). There were several substituents that displayed relative activities greater than what might be predicted based on their size (i.e. F, Me, and OMe). It was noticed that these three substituents had the common feature of all being net electron-donating groups, as indicated by their negative Hammett substituent constants, σ_p^+ (Hansch et al., 1991). This was in contrast

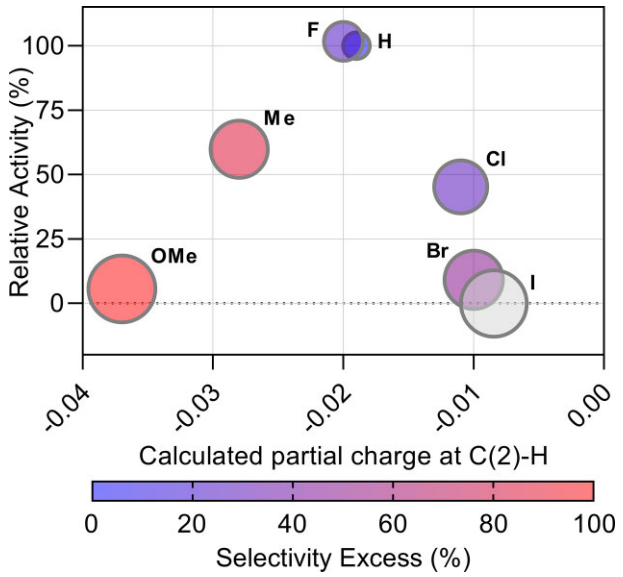

Fig. 7 Percentage relative activity of various 3-substituted benzoates as a function of calculated average partial charge at C(2)–H. The regioselectivity excess (%) is defined (major isomer – minor isomer)/(major isomer + minor isomer) × 100. The van der Waal's volumes (V_{vdW}) are reported as relative diameters and correspond to the following values in cubic angstrom: H, 5.06; F, 10.74; Cl, 19.94; Br, 24.19; I, 31.15; Me, 23.23; and OMe, 31.75.

to the other substituents, which possess positive σ_p^+ values (net electron withdrawing). For the purposes of comparison, the electronic contributions of the substituents are represented by the calculated Hirshfeld partial group charge at carbon 2 (Hirshfeld, 1977). As expected, the electron-donating substituents correlate to an increased partial charge at C(2)–H. In an attempt to incorporate both electronic and steric effects into interpretation of activity and selectivity, a plot was prepared that includes indicators of both size and selectivity for each substituent (Fig. 7). For the electron-donating substituents, there is a clear correlation between decreasing relative activity and increasing size. The trend is similar for the net electron-withdrawing substituents (i.e. Cl, Br, and I), but the relative decrease in activity appears more sensitive to size. The effect of electronics can best be seen by comparing substituents across similar levels of activity. For example, fluorine has twofold the V_{vdW} of hydrogen but maintains an activity that is equal to the native substrate. Comparison of the 3-Me substrate with the 3-Cl and 3-Br ones provides an even starker example of this disconnect between size and relative activity. Despite being larger than chlorine and nearly the same size as bromine, 3-methylbenzoate has a higher activity (15% and 50% greater, respectively). In this model, the lack of activity for 3-iodobenzoate can be directly attributed to its size, given the similarity of its partial C(2)–H charge to that of the other halogens. Similarly, the large volume of the 3-methyoxy substituent appears to be mitigated by its strong electron-donating capacity. When taken together, these results are consistent with those of Lipscomb, who identified electronic contributions to activity in studies with the isolated BZDO (Rivard et al., 2015).

Given the link between greater partial charge at C(2)–H and higher activities, we also wished to explore possible electronic effects on the regioselectivity of the reaction (Fig. 7). The selectivity for the 3-substituted diol over the 5-substituted diol (expressed as the regioselectivity excess) is higher for substrates bearing an electron-donating group compared with similarly sized substrates bearing electron-withdrawing groups. For example, 3-Me and 3-Br have a similar V_{vdW} (within 1 Å^3), but the 3-Me has a considerably larger bias toward the 3-substituted isomer. The 3-Fl and 3-Cl substrates have comparable regioselectivities, yet chlorine is nearly twice as large as fluorine. For the substrates that produce measurable quantities of both isomers (i.e. F, Cl, Br, and Me), the C-2 position being oxidized differs based on its arrangement relative to the substituent. The 3-substituted diol is derived from a C-2 that is *ortho* to the substituent, while the 5-substituted product has a carbon 2 (formally C-6) that is *para*. Examination of the partial charges of the C-2 versus C-6 positions failed to explain the preference for oxidation at C-2 (**Table S1**). The cause of this enhanced regioselectivity is therefore unclear. The most likely explanation is the existence of an unidentified active site interaction that either enhances selectivity for F, Me, and OMe or degrades it for Br and Cl. Given the dominant contribution of steric effects, it is likely that more substrates will need to be examined to fully describe the relationship between structure and reactivity in this BZDO system. This work is currently underway in our lab and will be reported in due course.

Conclusion

In summary, the application of quantitative ^{1}H-NMR spectroscopy has allowed for the rapid evaluation of a panel of monosubstituted benzoate substrates in *R. eutropha* B9 whole cells. The use of a single spectroscopic technique to characterize metabolites and quantify key biochemical components of the biocatalytic system makes this an attractive strategy for future studies involving BZDO and other RDDs. Given the synthetic importance of the *R. eutropha* B9 system, this will improve accessibility to non-native *ipso*,*ortho*-dihydrodiols for applications in synthesis.

Acknowledgments

We are grateful to Prof. Dalia Biswas, Whitman College, for performing calculations of the Hirshfeld partial group charges. We thank Prof. Tim Machonkin, Whitman College, for helpful conversations during the course of this work. This research was supported in part by Whitman College, the Whitman College Student/Faculty Summer Research Award Program, and the Murdock College Charitable Trust.

Supplementary Material

Supplementary material is available online at *JIMB* (*www.academic.oup.com/jimb*).

Authors' Contributions

J.C. designed and conceived research. J.B. and Z.C. conducted experiments. J.C. and J.B. analyzed data. J.C. wrote the manuscript with support from J.B. All the authors read and approved the manuscript.

Funding

This work was supported by a grant from the Murdock College Research Program for Natural Sciences (NS-201914176).

Conflict of Interest

The authors declare no competing interests.

Data Availability

All data are available upon reasonable request.

References

Adams, D. R., van Kempen, J., Hudlicky, J. R., & Hudlicky, T. (2014). Chemoenzymatic approach to synthesis of hydroxylated pyrrolidines from benzoic acid. *Heterocycles*, 88, 1255–1274. https://doi:10.3987/Com-13-S(S)89

Alexander, B. E., Sun, S., Palframan, M. J., Kociok-Kohn, G., Dibwe, D. F., Watanabe, S., Caggiano, L., Awale, S., & Lewis, S. E. (2020). Sidechain diversification of grandifloracin allows identification of analogues with enhanced anti-austerity activity against human PANC-1 pancreatic cancer cells. *ChemMedChem*, 15, 125–135. https://doi:10.1002/cmdc.201900549

Barding, G. A., Salditos, R., & Larive, C. K. (2012). Quantitative NMR for bioanalysis and metabolomics. *Analytical and Bioanalytical Chemistry*, 404, 1165–1179. https://doi:10.1007/s00216-012-6188-z

Barry, S. M. & Challis, G. L. (2013). Mechanism and catalytic diversity of Rieske non-heme iron-dependent oxygenases. *ACS Catalysis*, 3, 2362–2370. https://doi:10.1021/cs400087p

Brecker, L. & Ribbons, D. W. (2000). Biotransformations monitored *in situ* by proton nuclear magnetic resonance spectroscopy. *Trends in Biotechnology*, 18, 197–202. https://doi:10.1016/s0167-7799(00)01425-6

Charest, M. G., Lerner, C. D., Brubaker, J. D., Siegel, D. R., & Myers, A. G. (2005). A convergent enantioselective route to structurally diverse 6-deoxytetracycline antibiotics. *Science*, 308, 395–398. https://doi:10.1126/science.1109755

Collins, J. A., Gerry, C. J., & Duncan, M. M. (2019). A chemoenzymatic formal synthesis of epoxyquinols A and B. *Synlett*, 30, 2193–2197. https://doi:10.1055/s-0039-1690216

Ferraro, D. J., Gakhar, L., & Ramaswamy, S. (2005). Rieske business: Structure–function of Rieske non-heme oxygenases. *Biochemical and Biophysical Research Communications*, 338, 175–190. https://doi:10.1016/j.bbrc.2005.08.222

Fischer, T. M., Leisch, H., & Mihovilovic, M. (2010). Intramolecular Diels–Alder cyclization of biodihydroxylated benzoic acid derivatives towards novel heterocyclic scaffolds. *Monatshefte fur Chemie—Chemical Monthly*, 141, 699–707. https://doi:10.1007/s00706-010-0291-7

Froese, J., Overbeeke, C., & Hudlicky, T. (2016). Chemoenzymatic synthesis of pleiogenone A: An antiproliferative trihydroxyalkylcyclohexenone isolated from *Pleiogynium timorense*. *Chemistry—A European Journal*, 22, 6180–6184. https://doi:10.1002/chem.201601061

Ge, Y., Vaillancourt, F. H., Agar, N. Y., & Eltis, L. D. (2002). Reactivity of toluate dioxygenase with substituted benzoates and dioxygen. *Journal of Bacteriology*, 184, 4096–4103. https://doi:10.1128/jb.184.15.4096-4103.2002

Gibson, D. T., Koch, J. R., & Kallio, R. E. (1968). Oxidative degradation of aromatic hydrocarbons by microorganisms. I. Enzymic formation of catechol from benzene. *Biochemistry*, 7, 2653–2662. https://doi:10.1021/bi00847a031

Griffen, J. A., Le Coz, A. M., Kociok-Kohn, G., Khan, M. A., Stewart, A. J., & Lewis, S. E. (2011). Expanding the chiral pool: oxidation of *meta*-bromobenzoic acid by *R. eutrophus* B9 allows access to new reaction manifolds. *Organic & Biomolecular Chemistry*, 9, 3920–3928. https://doi:10.1039/c1ob05131h

Hansch, C., Leo, A., & Taft, R. W. (1991). A survey of Hammett substituent constants and resonance and field parameters. *Chem. Rev.*, 91, 165–195. https://doi: 10.1021/cr00002a004

Hirshfeld, F. L. (1977). Bonded-atom fragments for describing molecular charge densities. *Theoretica Chimica Acta*, 44, 129–138. https://doi:10.1007/BF00549096

Hudlicky, T. (1996). Design constraints in practical syntheses of complex molecules: current status, case studies with carbohydrates and alkaloids, and future perspectives. *Chemical Reviews*, 96, 3–30. https://doi:10.1021/cr950012g

Hudlicky, T. (2018). Benefits of unconventional methods in the total synthesis of natural products. *ACS Omega*, 3, 17326–17340. https://doi:10.1021/acsomega.8b02994

Jenkins, G. N., Ribbons, D. W., Widdowson, D. A., Slawin, A. M. Z., & Williams, D. J. (1995). Synthetic application of biotransformations: absolute stereochemistry and Diels–Alder reactions of the (1*S*,2*R*)-1,2-dihydroxycyclohexa-3,5-diene-1-carboxylic acid from *Pseudomonas putida*. *Journal of the Chemical Society, Perkin Transactions 1*, 1, 2647–2655. https://doi:10.1039/P19950002647

Johnson, B. F. & Stanier, R. Y. (1971). Regulation of the beta-ketoadipate pathway in *Alcaligenes eutrophus*. *Journal of Bacteriology*, 107, 476–485. https://doi.org/10.1128/jb.107.2.476-485.1971.

Johnson, R. A. (2004). *Microbial arene oxidations organic reactions*. John Wiley & Sons, Inc., pp. 117–264

Knackmuss, H. J. & Reineke, W. (1973). Der einfluss von chlorsubstituenten auf die oxygenierung von benzoat durch. *Chemosphere*, 2, 225–230. https://doi:10.1016/0045-6535(73)90045-3

Lewis, S. E. (2014). Applications of biocatalytic arene *ipso*,*ortho cis*-dihydroxylation in synthesis. *Chemical Communications*, 50, 2821–2830. https://doi:10.1039/c3cc49694e

Lewis, S. E. (2015). *Biotransformations of arenes arene chemistry*. John Wiley & Sons, Inc., pp. 913–937

Marenich, A. V., Cramer, C. J., & Truhlar, D. G. (2009). Universal solvation model based on solute electron density and on a continuum model of the solvent defined by the bulk dielectric constant and atomic surface tensions. *The Journal of Physical Chemistry B*, 113, 6378–6396. https://doi:10.1021/jp810292n

Myers, A. G., Siegel, D. R., Buzard, D. J., & Charest, M. G. (2001). Synthesis of a broad array of highly functionalized, enantiomerically pure cyclohexanecarboxylic acid derivatives by microbial dihydroxylation of benzoic acid and subsequent oxidative and rearrangement reactions. *Organic Letters*, 3, 2923–2926. https://doi:10.1021/ol010151m

Nash, T. J., Wharry, S., Moody, T. S., & Lewis, S. E. (2017). Biocatalytic dearomatisation of *para*-fluorobenzoic acid access to versatile homochiral building blocks with quaternary centres. *Chimica Oggi—Chemistry Today*, 35, 90–94

Neese, F. (2012). The ORCA program system. *WIREs Computational Molecular Science*, 2, 73–78. https://doi:10.1002/wcms.81

Neese, F. (2018). Software update: the ORCA program system, version 4.0. *WIREs Computational Molecular Science*, 8, e1327. https://doi:10.1002/wcms.1327

Pazos, M., Martínez, S., Vila, M. A., Rodríguez, P., Veiga, N., Seoane, G., & Carrera, I. (2015). Aza and oxo Diels–Alder reactions using *cis*-cyclohexadienediols of microbial origin: chemoenzymatic preparation of synthetically valuable heterocyclic scaffolds. *Tetrahedron: Asymmetry*, 26, 1436–1447. https://doi:10.1016/j.tetasy.2015.10.015

Reineke, W. & Knackmuss, H. J. (1978). Chemical-structure and biodegradability of halogenated aromatic-compounds—substituent effects on 1,2-dioxygenation of benzoic acid. *Biochimica et Biophysica Acta*, 542, 412–423. https://doi:10.1016/0304-4165(78)90372-0

Reineke, W. & Knackmuss, H. J. (1988). Microbial degradation of haloaromatics. *Annual Review of Microbiology*, 42, 263–287. https://doi:10.1146/annurev.mi.42.100188.001403

Reineke, W., Otting, W., & Knackmuss, H. J. (1978). *cis*-Dihydrodiols microbially produced from halo- and methylbenzoic acids. *Tetrahedron*, 34, 1707–1714. https://doi:10.1016/0040-4020(78)80206-3

Reiner, A. M. & Hegeman, G. D. (1971). Metabolism of benzoic acid by bacteria. Accumulation of (-)-3,5-cyclohexadiene-1,2-diol-1-carboxylic acid by mutant strain of *Alcaligenes eutrophus*. *Biochemistry*, 10, 2530–2536. https://doi:10.1021/bi00789a017

Rivard, B. S., Rogers, M. S., Marell, D. J., Neibergall, M. B., Chakrabarty, S., Cramer, C. J., & Lipscomb, J. D. (2015). Rate-determining attack on substrate precedes Rieske cluster oxidation during *cis*-dihydroxylation by benzoate dioxygenase. *Biochemistry*, 54, 4652–4664. https://doi:10.1021/acs.biochem.5b00573

Sambrook, J. & Russell, D. W. (2001). *Molecular cloning: a laboratory manual*. (3rd edn). Cold Spring Harbor Laboratory Press.

Simmler, C., Napolitano, J. G., McAlpine, J. B., Chen, S.-N., & Pauli, G. F. (2014). Universal quantitative NMR analysis of complex natural samples. *Current Opinion in Biotechnology*, 25, 51–59. https://doi:10.1016/j.copbio.2013.08.004

Sun, S.-Y., Zhang, X., Zhou, Q., Chen, J.-C., & Chen, G.-Q. (2008). Microbial production of *cis*-1,2-dihydroxy-cyclohexa-3,5-diene-1-carboxylate by genetically modified *Pseudomonas putida*. *Applied Microbiology and Biotechnology*, 80, 977–984. https://doi:10.1007/s00253-008-1603-2

Tan, W. A. & Parales, R. E. (2016). *Application of aromatic hydrocarbon dioxygenases green biocatalysis*. John Wiley & Sons, Inc., pp. 457–471

Wackett, L. P. (2002). Mechanism and applications of Rieske non-heme iron dioxygenases. *Enzyme and Microbial Technology*, 31, 577–587. https://doi:10.1016/S0141-0229(02)00129-1

Weigend, F. & Ahlrichs, R. (2005). Balanced basis sets of split valence, triple zeta valence and quadruple zeta valence quality for H to Rn: Design and assessment of accuracy. *Physical Chemistry Chemical Physics*, 7, 3297–3305. https://doi:10.1039/B508541A

Whited, G. M., Mccombie, W. R., Kwart, L. D., & Gibson, D. T. (1986). Identification of *cis*-diols as intermediates in the oxidation of aromatic acids by a strain of *Pseudomonas putida* that contains a TOL plasmid. *Journal of Bacteriology*, 166, 1028–1039. https://doi:10.1128/jb.166.3.1028-1039.1986

Wolfe, M. D., Altier, D. J., Stubna, A., Popescu, C. V., Munck, E., & Lipscomb, J. D. (2002). Benzoate 1,2-dioxygenase from *Pseudomonas putida*: Single turnover kinetics and regulation of a two-component Rieske dioxygenase. *Biochemistry*, 41, 9611–9626. https://doi:10.1021/bi025912n

Zhao, Y. & Truhlar, D. G. (2008). The M06 suite of density functionals for main group thermochemistry, thermochemical kinetics, noncovalent interactions, excited states, and transition elements: two new functionals and systematic testing of four M06-class functionals and 12 other functionals. *Theoretical Chemistry Accounts*, 120, 215–241. https://doi:10.1007/s00214-007-0310-x